Valence band photoemission from GaN(001) and GaAs:GaN-surfaces

T. Strasser, F. Starrost, C. Solterbeck, and W. Schattke
Institut für Theoretische Physik, Christian-Albrechts-Universität, Leibnizstr. 15, D-24098 Kiel, Germany
(July 28, 1997)

We present photoemission spectra calculated within the one-step model in normal emission from GaN and GaAs (001) surfaces. Structures in the spectra are discussed in terms of direct transitions from bulk valence states and as emissions from surface states, depending on polarization of the light. Thereby all of the pronounced structures in the energy distribution curves are uniquely associated with the participating bands and their orbital and layer resolved composition. The theoretical intensities are compared with experimental angle resolved ultraviolet photoemission spectra for clean GaAs and GaN surfaces yielding a good agreement. The comparison underlines the necessity of a full calculation for the interpretation of experimental data. In addition, we investigate the change in the calculated distribution curves introduced by covering a GaAs(001) substrate with several overlayers of GaN.

79.60.-i, 73.20.At, 73.61.Ey

I. INTRODUCTION

The most powerful experimental tool for examining the electronic structure of a semiconductor is the angle resolved ultraviolet photoemission spectroscopy (ARUPS). The spectra give insight into the valence band structure of the bulk as well as that of the surface, but simple analysis techniques allow only for a rough mapping of the bands. Beside the initial bound state, photoemission involves the excitation to outgoing scattering states with the transition probabilities given by matrix elements. Therefore, a full account of the experimental data can only be attained by a comparison with photocurrents calculated within the one-step model, which is the proper theoretical description.

Since the wide band gap semiconductor GaN offers exciting applications in optoelectronics, the electronic structure of GaN has gained strong experimental and theoretical interest. Although GaN usually crystallizes in the wurtzite structure, Yang et al. [1] have demonstrated that it is possible to grow cubic GaN on GaAs(001) surfaces, which promise enhanced electronic properties compared to the wurtzite phase. Furthermore GaN has been used for passivating the GaAs surface, e.g. by direct nitridation [2]. Actually, a variety of methods of growing cubic GaN on suitable substrates, as on SiC, is under investigation and techniques are rapidly evolving. Single growth mechanism are still open to question, e.g. the role of As as a surfactant [3].

At this stage the insight into the electronic binding from electronic spectroscopy is valuable for the choice of an effective preparation technique in addition to the basic understanding. As the already existing photoemission data show astonishingly good agreement with calculated bulk band structure of GaN, the theoretical decomposition of a spectrum into its contributions can explain microscopic electronic details which are responsible for establishing the geometrical surface configuration. Such a decomposition uses the flexibility in calculating the spectra by arbitrarily switching off perturbations which are not important for the main effects of interest. One is thus able to isolate the prominent binding mechanisms. E.g., it will be shown in the following that the full calculation within the one-step model safely allows to identify a structure as resulting from a surface state and not from a band edge as proposed in the original interpretation of the experiment. Therefore, the agreement of the experiment to ab initio calculations is closer than expected and presents itself as a guide to future investigations.

Apart from the bulk, the GaN layer growth on GaAs offers interesting problems. Because of the lattice mismatch deviations from planar interface configurations are observed for thicker films as well as smooth adjustments to the substrate in the case of thin films. To settle these questions it will be helpful to see what may be spectroscopically expected. To this end we calculated photoemission spectra also for the ideal GaAs(001)-(1x1) surface and its coverings with up to three layers of GaN in an ideal (1x1)-geometry. Thereby the transition from dispersive bulk induced spectra to extremely non dispersive curves is observed with increasing coverage.

The paper is organized as follow. First we give a short overview about the theory used in the calculations. Then we discuss the results for a GaN(001) surface, compare the photocurrent with experimental ARUPS data, and show how the various structures have to be interpreted. In a subsequent section the results for a clean GaAs(001) surface are presented in order to discuss the change in the photocurrent introduced by expitaxial GaN coverages. The GaAs results are tested on published experimental data. In the last part we examine the influence of GaN overlayers on clean GaAs(001) with respect to the electronic structure and the photocurrent.

II. THEORY

In this section, we briefly discuss the theoretical techniques used in the calculation of the photocurrent from semiconductor surfaces. For details see the references [4,5].

We calculate the photocurrent within the one-step model, based on the "golden rule" formulation of the photoemission process [7]. The photocurrent I is given by:

$$
\begin{aligned}
I \sim \sum_{i,j} & \langle \Phi^*_{LEED}(E_{fin}, k_{\|}) | \mathbf{A_0} \cdot \mathbf{p} | \Psi_i \rangle \\
& G_{i,j}(E_{fin} - h\nu, k_{\|}) \langle \Psi_j | \mathbf{p} \cdot \mathbf{A_0} | \Phi^*_{LEED}(E_{fin}, k_{\|}) \rangle
\end{aligned}
$$

The vectorpotential $\mathbf{A_0}$ is kept constant. $G_{i,j}$ represents the halfspace Green's function of the valence states, given in a layer resolved LCAO basis Ψ_i [8]. Our basis set consists of the 4s and 4p atomic orbitals of gallium and arsenic and the 2s and 2p atomic orbitals of nitrogen [13], taking into account the coupling up to fourth nearest neighbor atoms. The Hamilton matrix is calculated according to Extended-Hückel-Theory (EHT). Its parameters are adjusted to published ab initio bulk band structures using a genetic algorithm [9]. While the parameters are already known for GaAs [9], we determine them for GaN by adjusting to a GW calculation of the bulk band structure [10]. The result is shown in Tab. I and the bulk band structure of GaN is displayed in Fig. 1.

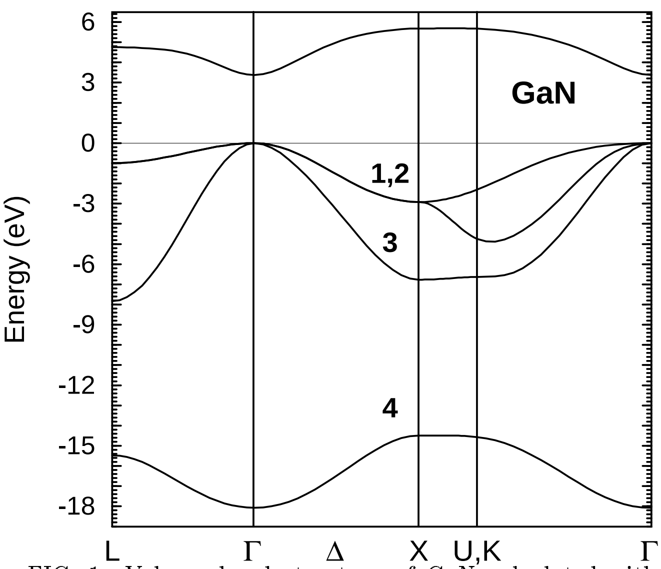

FIG. 1. Valence band structure of GaN calculated with EHT-parametrization acc. to Table I.

The electronic structure of the surface is determined by the calculation of the $\mathbf{k}_{\|}$-resolved density of states (DOS) from the Green's matrix, taking into account relaxation, reconstruction and adsorption at the surface. The resolution of the DOS with respect to atomic layers and orbital composition allows for a detailed characterization of the bands and their corresponding photocurrents.

The final state of photoemission is obtained as a scattering state with asymptotic boundary conditions. For a clean surface the wave function of the final state is determined by matching the solution of the complex bulk band structure [14,15] to the vacuum solution, representing the surface by a step potential. This treatment is best suited for discussing the photoemission peaks in terms of direct transitions with conservation of the surface perpendicular wave vector $k_{\perp}$ since the final state is described as a sum of solutions of the complex band structure for different $k_{\perp}$. The solution within the bulk is calculated by the empirical pseudopotential method, developed by Cohen and Bergstresser [11]. For GaAs we use the pseudopotential form factors of Ref. [11], while for GaN form factors of Fan et al. [12] are used. The damping of the wavefunction inside the crystal is described by the imaginary part of an optical potential. For treating overlayers like N or GaN on a GaAs surface, we introduce for the final states a simple potential well between the clean crystal and the vacuum region (see Fig. 2). The solutions of the three parts (crystal, well, and vacuum) are matched together at the two interfaces. The depth of the well is given by

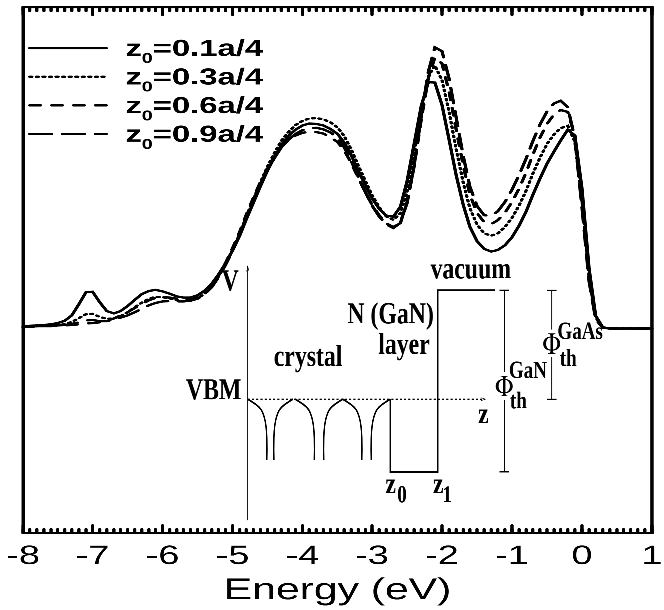

FIG. 2. Influence of the matching plane on the photocurrent of the GaN(001)-(1x1)Ga surface calculated for a photon energy of 44.0 eV insert: Model of a N (GaN) covered GaAs surface as used in the calculation the final states.

K_{ss}	K_{sp}	K_{pp}	I_{s0}	I_{p0}	$\tilde{I}_{s0}$	$\tilde{I}_{p0}$	I_{s1}	I_{p1}	$\tilde{I}_{s1}$	$\tilde{I}_{p1}$
1.0	0.844	0.844	54.66	39.94	20.49	7.76	24.28	21.19	13.82	4.71

TABLE I. EHT-parameter for GaN (0 means nitrogen and 1 gallium, for the notation see Starrost et al. [9]).

the work functions of GaAs (5.25 eV) and GaN (4.99 eV) [16].

In Eq. 1, the transition matrix elements $\langle\Phi^*_{LEED}(E_{fin}, k_{||})|\mathbf{A_0}\cdot\mathbf{p}|\Psi_i\rangle$ between the final state and the layer Bloch sums are calculated in real space, using good lattice points. These matrix elements are needed for a full analysis of the spectra. Their decomposition into the contributions from atomic layers and orbitals permits the discussion of the influence of the final states in relation to the characteristics of the initial states.

It should be mentioned that we use two different descriptions of the Hamiltonian for the initial and the final states. Such a description thoroughly adjusting the final state to photoemission [4,5] and targetcurrent [6] spectra, seems to account for the particle-hole many body problem on photoemission much better than simply taking initial and final states both from the same one-particle hamiltonian. For the many body transition amplitudes there is no orthogonality requirement.

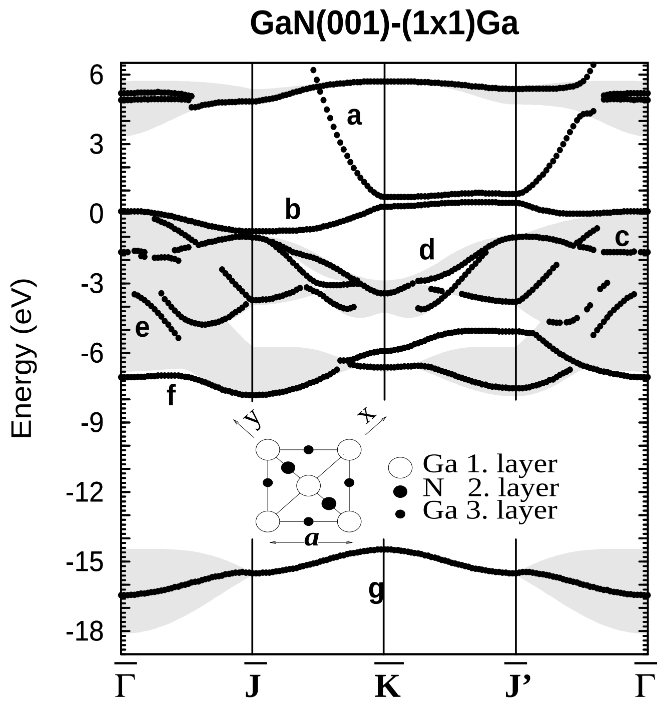

FIG. 3. Surface band structure of the GaN(001)-(1x1)Ga surface and the projected GaN bulk band structure (shaded). The insert shows the assumed ideal geometry (lattice constant a=4.5Å).

III. RESULTS AND DISCUSSION

A. GaN(001)-(1x1)Ga - Theory

In this section we discuss our results for an ideal Ga terminated GaN(001) surface. The geometry of the (1x1) surface is given in Fig. 3 together with the surface band structure. We find several resonances and surface states. Within the fundamental gap there are two states which can be identified as a bridge (a) and a dangling bond (b) state. The bridge bond is built up by Ga p_x-orbitals, while the last one changes its orbital composition. In $\overline{\Gamma}$ (b) is made up of Ga p_z- and s-orbitals with strong contributions from the underlying nitrogen p_z-orbitals while at $\overline{K}$ the nitrogen p_y-orbitals contribute. It has to be noted that the dangling bond state is in resonance with the bulk along $\overline{\Gamma}$-$\overline{J}$ as well as along $\overline{\Gamma}$-$\overline{J'}$. For higher binding energies we find back bond states, e.g. the resonance (c) at -1.8 eV, which can be seen as a broad structure in the layer resolved density of states in $\overline{\Gamma}$ (Fig. 4). We find in Fig. 4 contributions from the uppermost nitrogen p_x-and p_y-orbitals as well as weak contributions from the Ga p_y-orbitals, indicating the bond between the gallium and nitrogen atoms. Near the heteropolar gap (Fig. 3) we see Ga s-states labeled by (f) with contributions from the N p_z-orbitals at $\overline{\Gamma}$ and N p_x as well as p_y-orbitals at $\overline{K}$. Below the heteropolar gap, we find a nitrogen s-state localized around -16 eV. This interpretation of the density of states is in good agreement with an ab initio pseudopotential calculation of Jhi and Ihm [17].

The complex final state bands are shown in Fig. 5. They are calculated along the symmetry line Δ which corresponds to normal emission. All bands are damped because of the imaginary part of the optical potential. The lengths of the bars denote the weight which single complex bands carry in the final state. Not all bands are important for the photoemission. We find three bands, which contribute strongly to the final state (labeled by (a), (b) and (d)). Especially the complex band (d) shows large expansion coefficients. Together with band (b) it

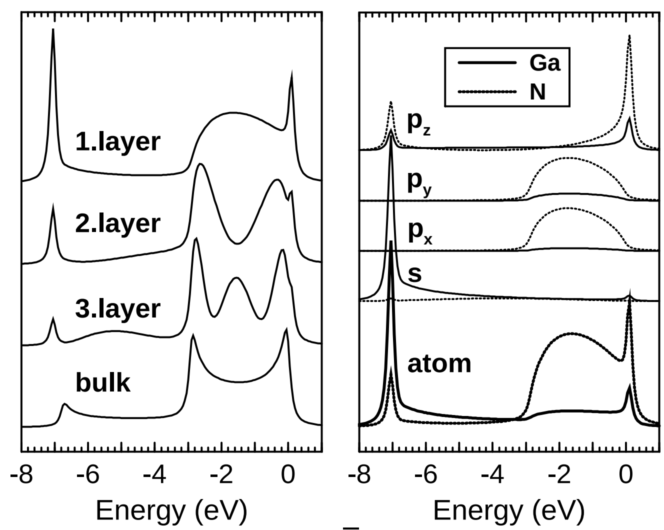

FIG. 4. Density of states at $\overline{\Gamma}$ for GaN(001)-(1x1)Ga. On the left hand side the layer resolved DOS is shown, while on the right the DOS of the first layer is further resolved into its atomic and orbital contributions. A layer comprises a Ga and N double plane.

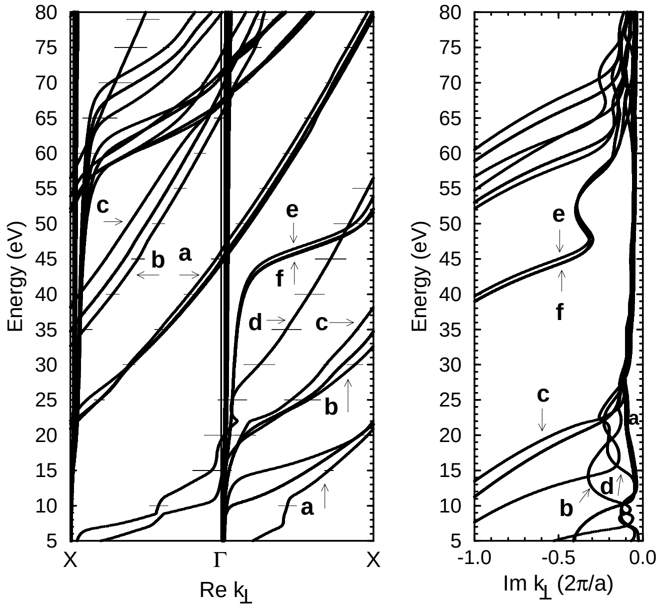

FIG. 5. Complex band structure of GaN for the symmetry line Δ. Bars indicate the magnitude of the expansion coefficients of the final state with respect to the complex bulk bands.

presents large imaginary parts for final state energies below 28 eV yielding a strong decrease of the states from the surface into the crystal.

Fig. 6 presents normal emission spectra for the GaN(001)-(1x1)Ga surface, which are calculated for photon energies from 10 up to 80 eV. The radiation is chosen to be incident in the yz plane, at an angle of 45° to the surface normal. First, we consider parallel polarized light, while the spectra for unpolarized light will be discussed subsequently. The matching plane is put at 0.7a/4 above the topmost Ga atom (Fig. 2 shows the small influence of the position of the matching plane on the photocurrent). We find in the spectra several structures which disperse with photon energy. Especially for photon energies above 30 eV, the structures can be interpreted by assuming direct transitions, i.e. with exact conservation of the perpendicular wave vector. For a given excitation energy we determine the binding energy at which transitions into the complex conduction band structure are possible and indicate these positions in the spectra by bars, see Fig. 6. The correspondence between peaks of subsequent spectra is achieved by structure plots, in which one combines a valence band with a conduction band and maps the energetic difference, i.e. the photon frequency, continuously onto the binding energy.

The structures (a) and (b) in Fig. 6 are explained by direct transitions from the valence bands denoted in Fig. 1 as (1,2) and (3), respectively, into the final state labeled by (d) in Fig. 5. The lack of dispersion of (a) between 15 eV and 29 eV photon energy can be explained by the small dispersion of the valence band (1,2) in combination with the almost vertical slope of the final band (d). At these energies, direct transitions into (d) arise only from $k_\perp$ in the vicinity of Γ. Additionally, the large imaginary part of the final band (d) for final state energies smaller than 28 eV causes a strong concentration of the wave function at the surface. This damps the influence of possible dispersive bulk bands. Above 28 eV final state energy the photoemission spectra are dominated by the same but now dispersive structures (a) and (b), which is consistent with the small imaginary part and the large expansion coefficient of the final band (d).

Below 30 eV photon energy there are two weak structures (c) and (d) with dispersion, which belong to transitions from the valence band (1,2) and (3), respectively, into the final band (a). The high dispersion in the final band (a) for energies between 10 and 13 eV results in the non dispersive structure at 1.4 eV binding energy for photon energies below 13 eV. Above 30 eV photon energy it is difficult to follow these structures, because a crossover occurs to the more intense emissions from the final band (d) discussed above. The remaining dispersive structures (e) and (f) can be seen for photon energies down to 26 and 28 eV, respectively. Structure (f) can only be followed up to photon energies of 35 eV, while structure (e) can be seen up to 80 eV. These latter peaks can be explained by direct transitions into the final band (b), which leaves the region of strong final state damping above 28 eV.

Besides the dispersive structures, we find two sequences of peaks without dispersion in Fig. 6. The first one is localized near the valence band maximum (VBM) and is labeled by (a'). Partly it coincides with (a). According to the DOS at $\overline{\Gamma}$ (see Fig. 4) we expect emissions from the gallium and nitrogen p_z-orbitals. Examining the matrix elements shown in Fig. 7, emissions from gallium p_z-orbitals for photon energies below 20 eV and less pronounced between 20 and 35 eV are favourized, while the matrix elements of nitrogen p_z-orbitals are significant between 10 and 20 eV and above 40 eV. Because the emissions from these orbitals are mixed with direct transitions from the VBM, as discussed above, the dangling bond state can only be seen as a small shoulder for photon energies below 14 eV and between 31 and 35 eV. Above 40 eV the emissions have to be attributed to nitrogen p_z-orbitals.

The second non dispersive series of peaks (g) at an energy of -7.1 eV are emissions from the Ga s-orbitals, which can be seen by a huge peak in the density of states of the three uppermost layers in Fig. 4. With increasing photon energy the emissions show a strong modulation in intensity, which stem from the matrix elements, as can be seen in Fig. 7. Especially the decreasing intensity around 44 eV photon energy can be traced to the minimum in the Ga s-orbital matrix element at 34 eV final state energy. For higher photon energies one has also to consider possible emissions from the nitrogen p_z-orbitals, which show enhanced matrix elements above 40 eV final

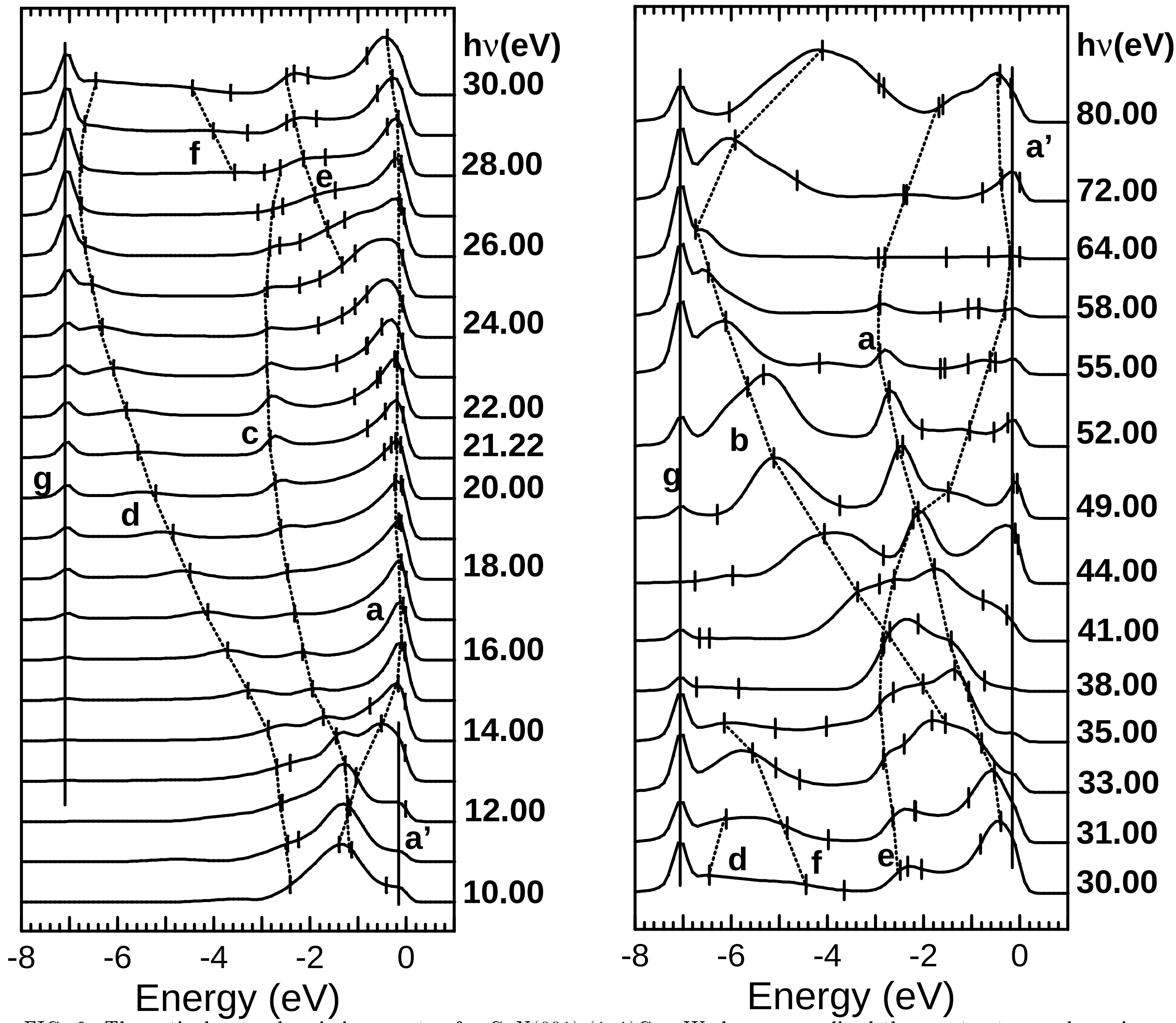

FIG. 6. Theoretical normal emission spectra for GaN(001)-(1x1)Ga. We have normalized the spectra to equal maximum photocurrent. The bars indicate binding energies at which direct transitions would be positioned. Their dispersion, which is discussed in the text, is traced via structure plots and drawn by dotted lines. Solid lines denote surface states. The zero energy is the VBM, the light is chosen incident along the yz plane with p-polarization. The excitation energies are indicated on the right of each picture and the letters are used for reference in the text.

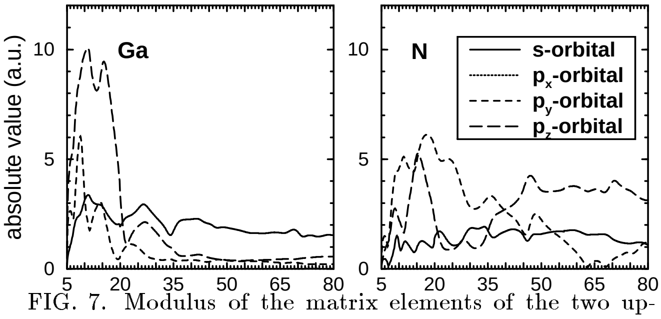

FIG. 7. Modulus of the matrix elements of the two uppermost atomic layers of the GaN(001)-(1x1)Ga surface resolved into orbitals. The matrix elements are calculated for p-polarized light incident in the yz plane. Only the orbitals plotted here contribute to the current because of selection rules.

state energy. The emissions from the dispersive structure (c) for photon energies between 20 and 25 eV are substantially enhanced in rotating the incidence direction of the light from the yz plane into the xz plane. In accordance with the orbital matrix elements of the first layer the emissions result from about 2.7 eV binding energy.

In the next step we use unpolarized radiation incident along the yz plane. This enhances the emissions from the p_x-orbitals. The photoemission spectra for photon energies above 30 eV shown in Fig. 8 display all those features of Fig. 6 and can be similarly discussed. E.g. the structure (a) can be identified and supports the interpretation of that peak given in the context of Fig. 6.

Summarizing the above discussion, we have shown that also dispersive structures, via direct transitions clearly attributed to bulk valence bands, are strongly affected by the surface through the complex band structure. Moreover, we could identify contributions from single layers and orbitals. Furthermore, remarkable energetic shifts of the peak positions relative to the band energies occur, which would make a band mapping fail severely.

B. GaN(001)-(1x1)-Comparison with Experiment

Recently Ding et al. [18] have grown GaN(100) samples by plasma-assisted MBE on GaAs(100) substrates. Their sample show a (1x1) LEED pattern with a strong diffuse background. They analyzed the samples with angle resolved photoemission in normal emission for photon energies between 31 and 80 eV. Excellent agreement between their experimental data and our theoretical results is found, as shown in Fig. 8. For example, theory and experiment observe the Ga s-related peak at -7.0 and -6.8 eV respectively. Both results agree in the decreasing intensity of this structure for photon energies around 44 eV. This clear coincidence is not a feature often seen in the comparison of theoretical and experimental semiconductor spectra. It confirms also the adequacy of the final state bands, which are the most difficult ingredient in a photocurrent calculation. Different from the experimental suggestion we attribute this peak to strong surface emissions rather than to indirect transitions from X_3, because the X_3 band edge appears at slightly higher energies according to Fig. 4 and is not seen in theory. Furthermore, theory shows with peak (b) a strong dispersive structure from -2.5 to -6.5 eV for photon energies between 38 and 64 eV, which can be clearly identified with a corresponding peak in experiment. At lower binding energy the experimental spectra show a second dispersive structure, which can be related to the structure (a) in the theoretical spectra. The rather flat behavior for excitation energies 58 and 64 eV between 0 and -5 eV of the experimental spectra is also reproduced by theory, especially for 64 eV.

The comparison between the theoretical and experimental spectra shows how bandmapping methods may fail. The theoretical peak (a) shows highest binding energy at $h\nu$=58 eV with $E_b \approx$2.8 eV. Its dispersion is connected with the bulk band $\Delta_{(1,2)}$ and its band edge X_5 is thus found around 58 eV photon energy. Considering the experimental curve for this frequency the broad maximum in the low binding energy range would allow for any energy between the marks at that curve. Moreover, the 72 eV spectrum shows a maximum (not marked) near 3 eV in agreement with theory. All this indicates that contrary to experimental peak deconvolution techniques the band edge X_5 may in fact coincide with the binding energy predicted by actual band structure calculations on which the present theoretical analysis relies.

A further remark refers to the experimental structure marked in the range of -3 to -4 eV within the spectra between $h\nu$ =49 eV and 80 eV. According to the theoretical results direct transitions are expected at $h\nu$ =49 eV, E_b =-3.8 eV, at $h\nu$ =55 eV, E_b =-4.2 eV, at $h\nu$ =72 eV, E_b =-4.7 eV, and at $h\nu$ =80 eV, E_b =-4.1 eV, of which only the last shows the intensity found in the experiment. Except for the last structure these emissions originate from valence band (3) and transitions to final states with significantly smaller coupling to the escaping electrons (final states (b), (c) and (a), see Fig. 5). The experiment shows a rather large background in this energy region. One might attribute the experimental marks to these direct transitions, if one neglects that the theoretical results partly underestimate the intensity. The inverse behavior occurs for the nitrogen p_z surface state seen at (a') in the theoretical spectra which appears to be suppressed in the experiment. In both cases the difference in intensity may be due to a surface contamination or to a surface geometry deviating from the assumed ideal bulk configuration.

The direct assignment of theoretical band energies vs. $k_\perp$ along Γ-X from the experimental spectra depends critically on the choice of final states. A misleading association of $k_\perp$ may occur. However, in this case the foregoing theoretical analysis shows that the dispersive structures

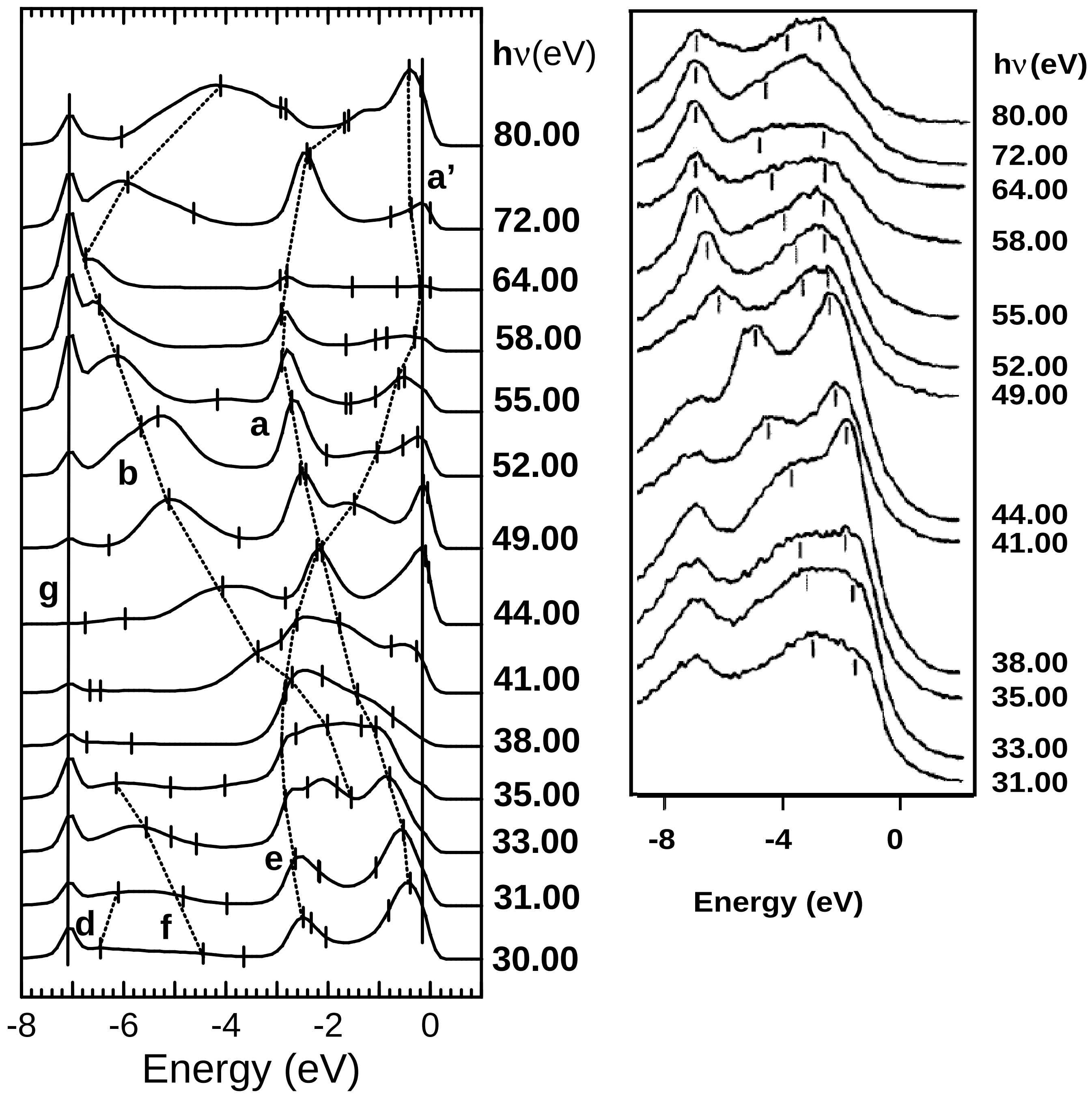

FIG. 8. Theoretical photoemission spectra in normal emission for GaN(001)-(1x1)Ga with unpolarized light incident in the yz plane, for further details see Fig. 6. On the right hand side, experimental spectra by Ding et al. are shown [18]. Markers in the experimental spectra indicate peak positions used in the experimental band determination.

are occasionally determined by one final state band, denoted by (d) in Fig. 5. Only then the simplified experimental analysis with one final state parabola is justified if one concedes a respective error bar at the derived bands.

C. GaAs(001)-(1x1)Ga

In order to discuss GaN overlayers on GaAs(001) we consider first a calculation for the pure GaAs(001) surface and compare it with GaN(001). For this aim the surface is assumed to be ideal and gallium terminated and the geometry is chosen as for the GaN surface (see Fig. 3). In Fig. 9 we show the surface band structure for the GaAs(001) surface. The electronic structure is similar to that of GaN. In the fundamental gap there is a bridge bond state (a), localized at the first layer Ga p_x-orbitals, and a dangling bond state (b), with an orbital composition similar to its counterpart of the GaN(001) surface. Because of the lower orbital energy of the nitrogen atom and the resulting reduced extension of the wavefunction compared to the arsenic atom, the bands within the fundamental gap of GaN show less dispersion than in the GaAs case. The resonances (d) and (c) consist of contributions of gallium and arsenic p-orbitals representing back bond states. Near the lower valence band edge we find Ga s-states, similar in energy to their counterpart at the GaN surface, but in contrast to GaN the Ga s states of the GaAs(001) surface remain resonance's residing close to the border of the stomach gap. Below the heteropolar gap an As s- surface state appears, which is to be compared with the N s states at lower binding energy according to the lower nitrogen orbital energy. The surface band structure is in good agreement with theoretical results from Ivanov et al. [20].

Similar to GaN we find in the complex band structure of the GaAs(001) surface (not shown here) a band that shows strong contributions to the final state. The complex bands for GaAs have large imaginary parts for energies lower than 15 eV, whereas with GaN large imaginary parts already arise for energies lower than 28 eV.

Fig. 10 shows the spectra in normal emission for the GaAs(001)-(1x1)Ga surface calculated for photon energies from 10 up to 30 eV. The plane of incidence of the light is the yz plane and the light is polarized parallel to this plane with a polar angle of 45°. We find six dispersive structures in the spectra which are explained by direct transitions. The two dispersive structures (d) and (b) are explained by direct transitions from the GaAs valence bands (3) and (1,2) (notation as in Fig. 1) to the same final state band. Because the latter shows the largest coefficients in the expansion of the LEED state pronounced emissions from these transitions appear for higher photon energies. We compare these results to those for the GaN surface. There, pronounced dispersive structures can only be seen for final state energies

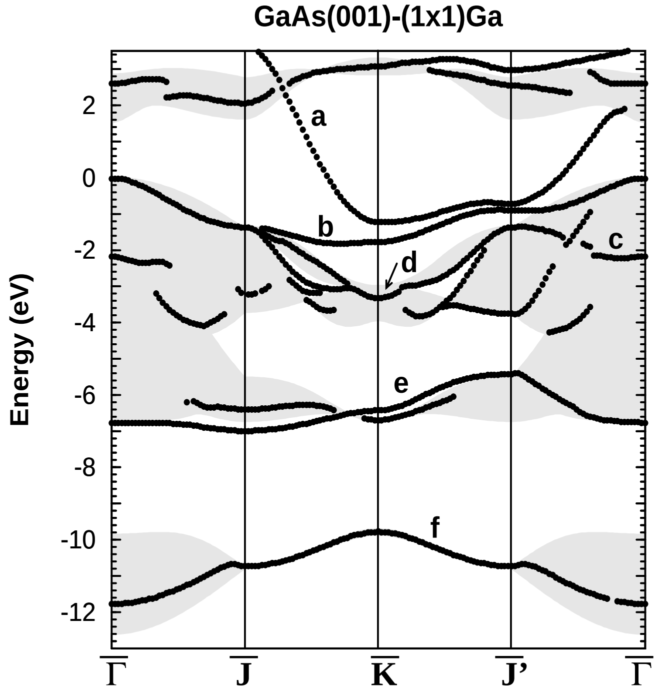

FIG. 9. Surface band structure of the GaAs(001)-(1x1)Ga surface and the projected bulk band structure of GaAs (shaded).

above 30 eV. This difference stems from the large imaginary parts of the wavevector for GaN at final state energies below 30 eV. The final states quickly decrease inside the crystal and yield small matrix elements. For GaAs the large imaginary parts of the relevant final states are reduced for final state energies above 14 eV and the strong dispersive structure (b) clearly appears in the spectra.

The remaining dispersive structures ((c), (e), (f), and (g)) can be explained by direct transitions in different final bands, which contribute less to the final state. As in the case of GaN their visibility can be discussed by the characteristics of the final bands. The high DOS at the valence band edge at X, i.e. -2.8 eV, extends from the bulk up to the second layer and can be seen in the theoretical spectra around 23 eV photon energy mixed with the direct transitions (c). This peak is related to p_x- and p_y-orbitals, forming the gallium-arsenic bond.

Furthermore, emissions from the dangling bond state near the valence band edge are less pronounced than in the GaN case, which is consistent with the differences in the DOS for both systems. The GaAs dangling bond contributes less to the DOS than its GaN counterpart. The absence of strong emissions from the Ga s states at the lower valence band edge is explained by the matrix elements of the Ga s-orbitals for the GaAs surface which are smaller than those for the GaN surface by a factor of 3.

Olde et al. [21] have investigated the photocurrent from a GaAs(001)-c(4x4) surface and have found strong

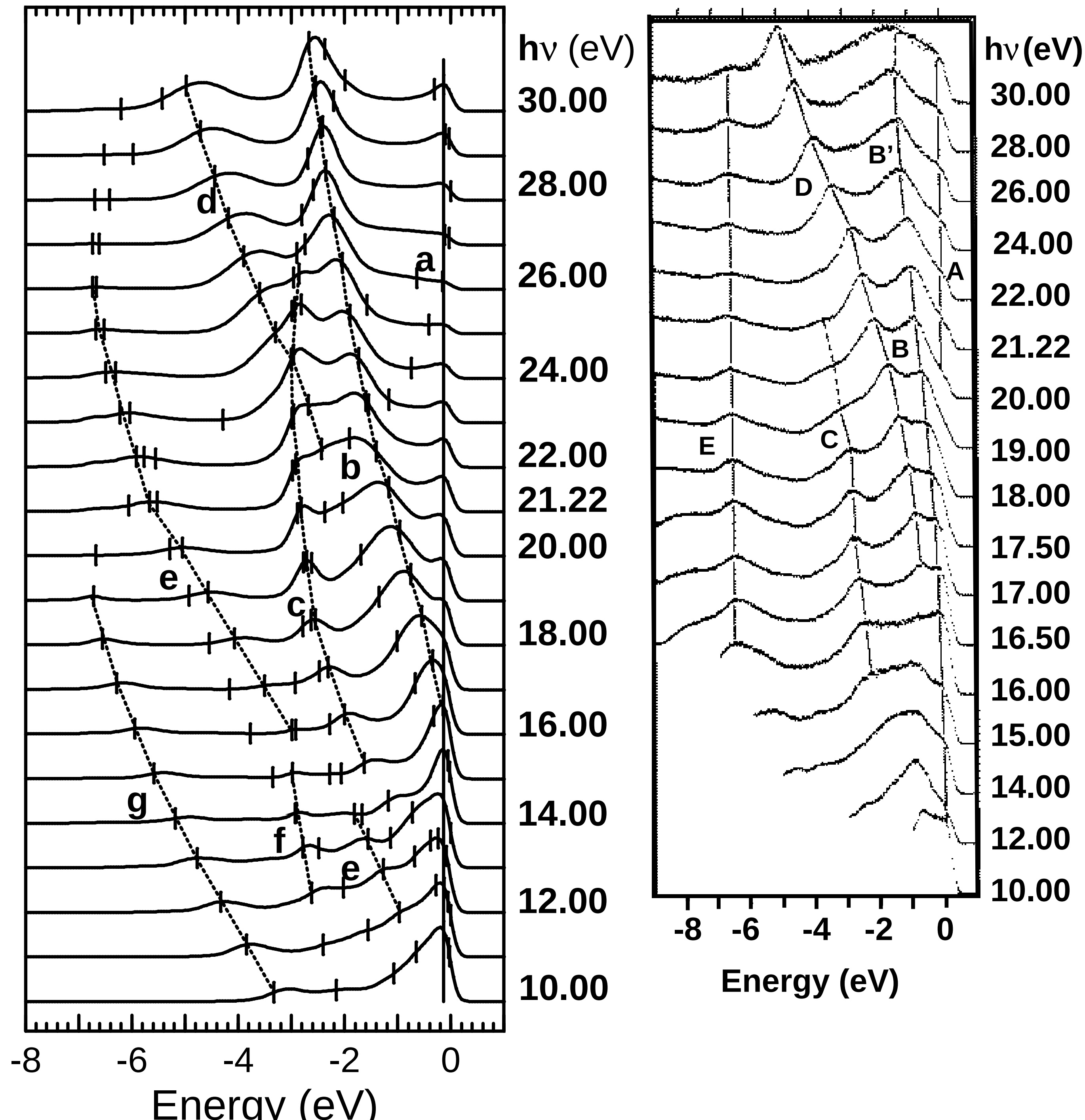

FIG. 10. Left hand side: Theoretical photoemission spectra in normal emission for GaAs(001)-(1x1)Ga, for details see Fig. 6. Right hand side: Experimental spectra in normal emission for GaAs(001)-c(4x4), taken from Olde et al. [21]

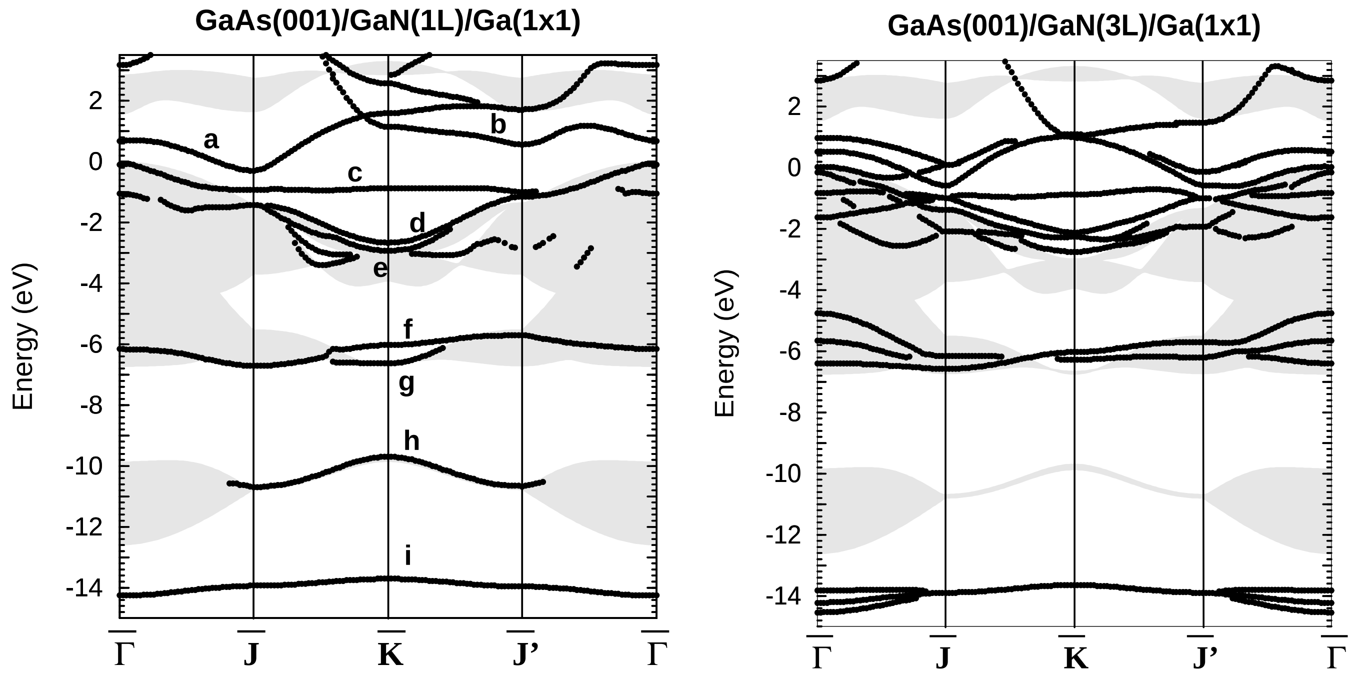

FIG. 11. Surface band structures for the systems GaAs(001)/GaN(1L)/Ga(1x1) and GaAs(001)/GaN(3L)/Ga(1x1) shown together with the projected GaAs bulk band structure.

dispersive features, which have been attributed to direct transitions. Despite the different surface geometry we find a good agreement with the strong features of the experimental results. Especially the structures (b), (c) and (d) in the theoretical spectra have their experimental counterpart in (B), (C) and (D). At first glance differences appear with regard to the experimental peak (E). However, up to 17 eV photon energy we interpret this peak being associated with the theoretical peak (g), especially because a dispersion in the lower frequency range seems to be present. Above 17 eV a dispersionless transition from the surface Ga *s*-orbital is found in theory, but as already discussed the matrix element is too small to appear in the spectrum, perhaps due to the different surface reconstruction. The differences in the energetical position of the states (b) and (B') for photon energies above 26 eV confirm the experimental interpretation that this peak stems from a surface state than bulk related. Of course, this surface state can not be expected in our calculation because of the different reconstruction. Usually surface emissions dominate the bulk emissions through their matrix elements, so the direct transition (b) in theory is hidden in the experimental surface peak around -1.5 eV. We note that this analysis is the first one-step calculation for this surface. It shows a satisfactory agreement of the bulk features.

D. GaAs(001)/GaN(xL)/Ga(1x1)

In this part we investigate GaAs(001) surfaces, which are covered by one to three GaN overlayers. We assume

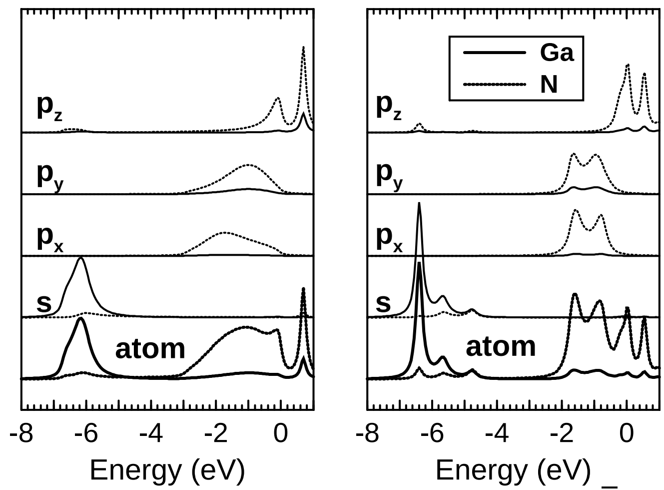

FIG. 12. Density of states for the first layer at $\overline{\Gamma}$ for GaAs(001)/GaN(xL)/Ga(1x1) resolved into its atomic and orbital components (on the left hand side x=1 and on the right hand side x=3)

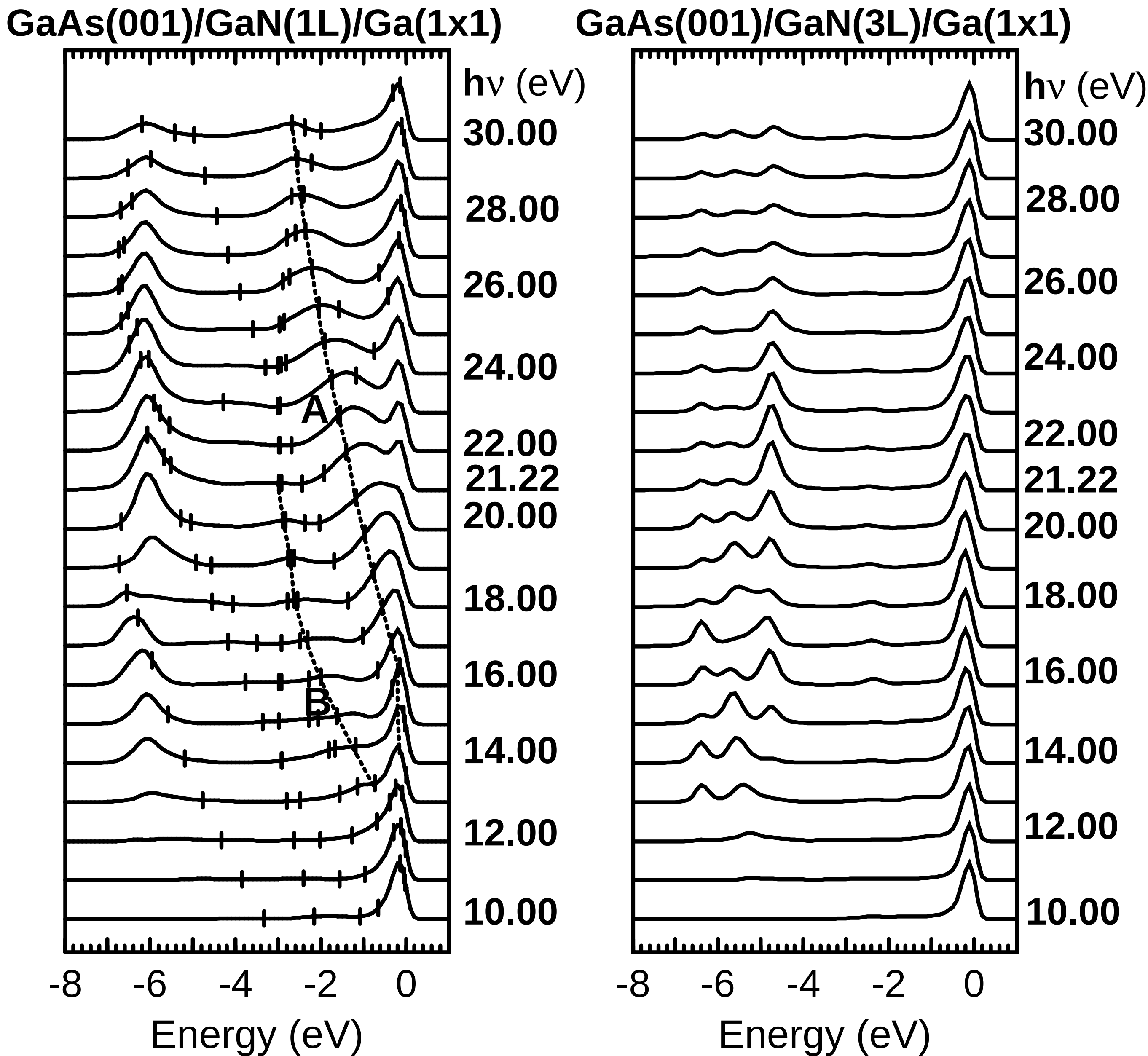

FIG. 13. Photoemission spectra in normal emission from GaAs(001) surface covered by one and three layers of GaN. The light is chosen being incident in the yz plane with p-polarization. For details see Fig. 6.

that GaN layers are continue the ideal GaAs crystal without relaxation or reconstruction. The uppermost plane is chosen to be gallium terminated with the geometry chosen as sketched in Fig. 3. Fig. 11 shows the calculated surface band structures for two such systems. Additional layers of GaN yield an increasing number of surface states and resonances. This is seen at the lower valence band edge with Ga s states, or at -14 eV with N s states. Within the fundamental gap we find for the system GaAs(001)/GaN(1L)/Ga(1x1) at $\overline{\mathrm{K}}$ a gallium p_x (a), a nitrogen p_x (b) and a hybridized gallium p_z - nitrogen p_y state (c). The surface bands (a) and (c) change their orbital composition in $\overline{\Gamma}$ and become gallium and nitrogen p_z dominated. The states between the upper valence band edge and the stomach gap are made up of contributions from the nitrogen as well as from the gallium p_x- and p_y-orbitals. In $\overline{\mathrm{K}}$ we find also contributions from the nitrogen p_z-orbitals. The layer resolved DOS is displayed in Fig. 12 for the first layer. The contributions from the Ga s orbitals near the heteropolar gap are distributed over all GaN layers, split in energy, and varying in density with the orbital's distance from the surface.

Fig. 13 shows the calculated photoemission spectra for both systems. For one overlayer of GaN we find two dispersive structures ((A) and (B)), which can be related to direct transitions from the GaAs bulk bands (1,2) (notation as in Fig. 1). The strong emissions related to transitions from the valence band (3), which appear as a feature labeled by (d) in the spectra of the clean GaAs surface (see Fig. 10), are missing here. That is despite the fact that the weight the corresponding complex band contributes to the final state is nearly unchanged (not shown here). Instead, the Ga p_z matrix element of the first atomic layers increase by a factor of three compared to the clean surface and rapidly decrease towards the interior. This may enhance the influence of the surface to the photocurrent hiding the dispersion found in Fig. 10. At -6.0 eV we find the emissions from the Ga s orbitals, modulated in their intensity by the Ga s-related matrix elements as shown in Fig. 14. The minimum in the intensity of these emissions at a photon energy of 18 eV can be explained by the minimum in the Ga s-matrix elements at 12 eV final state energy. Simultaneously the matrix elements of the nitrogen p_z- and of the Ga s-orbitals (not shown) of the second layer reach their maximum, such that one observes a weak emission from the small nitrogen p_z DOS as well as from Ga s at -6.5 eV for that excitation energy. This change in intensity of contributions from single orbitals is responsible for the fake dispersion of the surface peaks near -6 eV for photon energies between 15 and 19 eV. The emissions near the VBM are associated with nitrogen and gallium p_z-orbitals. The small DOS of the latter is compensated by large matrix elements.

Covering the surface with a second and a third layer of GaN, the dispersive structures disappear entirely and

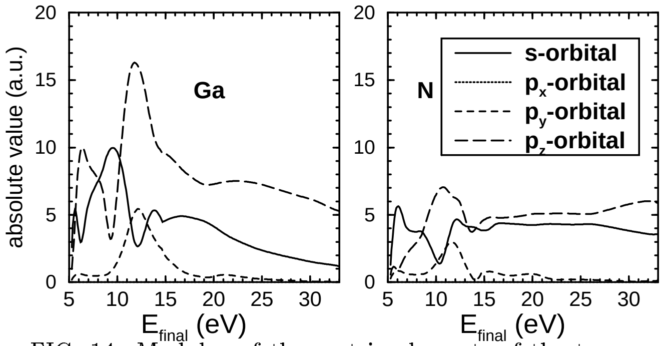

FIG. 14. Modulus of the matrix elements of the two uppermost atomic planes of the GaAs(001)/GaN(1L)/Ga(1x1) surface.

the spectra are dominated by the strong emissions from the upper gallium- and nitrogen p_z-orbitals at the VBM. Additionally we observe an increasing number of emissions from the Ga s-orbitals at highest binding energies. For the system GaAs(001)/GaN(2L)/Ga(1x1) (not shown here) emissions at -5.1 eV are related to Ga s-orbitals, which are localized in the second layer, while emissions from -6.4 eV are from Ga s-orbitals of the first layer. For the system GaAs(001)/GaN(3L)/Ga(1x1) the Ga s-emissions at highest binding energy again represent emissions from the first layer Ga, while the peaks at -4.8 eV belong to emissions from the second layer, and the structure between can be explained by emissions from the third layer. Furthermore we see for the GaAs(001)/GaN(2L)/Ga(1x1) surface weak emissions near -3.0 eV and for the GaAs(001)/GaN(3L)/Ga(1x1) surface weak emissions near -2.4 eV. Both structures are emissions from the Ga and As p_x- and p_y-orbitals indicating the binding between the Ga and As atoms just below the lowest N layer. As a consequence, the peak is rather faint. Decreasing intensity with emission depth usually is accepted as a rule. However, the splitted peak around -5 eV shows for $h\nu = 15$ eV that even the third layer can yield important contributions.

IV. CONCLUSION

Photoemission spectra in normal emission for the GaN(001) surface have been calculated within the one-step model. The spectra show several dispersive structures, which can be attributed to direct transitions from the valence into the final bands though peaks are generally shifted. Particularly for photon energies above 30 eV the spectra exhibit strong dispersive structures. This is an effect of the dispersion and damping of the final bands. Furthermore, we have identified emissions from surface states and resonances like the dangling bond. The calculated spectra not only reproduce properties of the experimental spectra, like dispersion and intensities, moreover they allowed us to clarify failures of the band mapping used in the experimental interpretation of the spectra.

In addition theoretical photoemission spectra for GaAs(001) have been determined showing also strong dispersive structures. In contrast to the GaN spectra, pronounced dispersion is also observed for photon energies below 30 eV excitation energy. We attribute these differences mainly to the complex band structures. The result agrees well with an experiment performed on a different surface reconstruction as far as the bulk emissions are concerned.

Covering the GaAs(001) surface with GaN several non dispersive structures are found, which can be related to the density of states, e.g. to the dangling bond and the Ga s-orbitals of the single overlayers. The number of non dispersive peaks increases with the number of overlayers as it should. However, even with three overlayers of GaN one can still identify emissions from the hidden Ga-As bond.

Summarizing the details of the discussion we conclude that with the help of a full theoretical analysis within the one-step model a lot of important information can be extracted from the experimental data. This is far more than contained in merely stating good agreement between an experimental and a theoretical set of curves.

V. ACKNOWLEDGMENTS

Part of this paper was prepared during an STA fellowship of one of the authors at the Joint Research Center for Atom Technology in Tsukuba. The hospitality of Prof. K. Terakura is gratefully acknowledged. The work was supported by a grant of the Land Schleswig-Holstein.

[1] H. Yang, O. Brandt, and K. Ploog, Phys. Status Solid (B) **194**, 109 (1996).

[2] Y. Bu and M.C. Lin, Surf. Sci. **317**, 152 (1994).

[3] G. Feuillet, H. Hamaguchi, K. Ohta, P. Hacke, H. Okumura, and S. Yoshida, Appl. Phys. Lett. **70**, 1025 (1997).

[4] J. Henk, W. Schattke, H.-P. Barnscheid, C. Janowitz, R. Manzke, and M. Skibowski, Phys. Rev. B **39**, 13286 (1989).

[5] J. Henk, W. Schattke, H. Carstensen, R. Manzke, and M. Skibowski, Phys. Rev. B **47**, 2251 (1993).

[6] J.-V. Peetz, W. Schattke, H. Carstensen, R. Manzke, and M. Skibowski, Phys. Rev. B **46**, 10127 (1992).

[7] P. J. Feibelman and D. E. Eastman, Phys. Rev. B **10**, 4932 (1974).

[8] J. Henk and W. Schattke, Comput. Phys. Commun. **77**, 69 (1993).

[9] F. Starrost, S. Bornholdt, C. Solterbeck, and W. Schattke, Phys. Rev. B **53**, 12549 (1996); **54**, 17226 (1996).

[10] A. Rubio, J. L. Corkill, M. L. Cohen, E. L. Shirley, and S. G.Louie, Phys. Rev. B **48**, 11810 (1993).

[11] M. L. Cohen and T. K. Bergstresser, Phys. Rev. B **141**, 789 (1966).

[12] W. J. Fan, M. F. Lin, T.C. Chong, and J. B. Xia, J. Appl. Phys. **79**, 188 (1996).

[13] E. Clementi and C. Roetti, At. Data Nucl. Data Tables **14**, 177 (1974).

[14] H. Bross, Surf. Sci. **213**, 215 (1989).

[15] J. B. Pendry, J. Phys. C **2**, 2273 (1969).

[16] D. Troost, H.-U. Baier, A. Berger, and W. Mönch, Surf. Sci. **242**, 324 (1991).

[17] S.-H. Jhi and J. Ihm, Phys. Status Solidi (B) **191**, 387 (1995).

[18] S. A. Ding, G. Neuhold, J.H. Weaver, P. Häberle, K. Horn, O. Brandt, H. Yang, and K. Ploog, J. Vac. Sci. Technol. A **14**, 819 (May/Jun 1996).

[19] V. Fiorentini, M. Methfessel, and M. Scheffler, Phys. Rev. B **47**, 13353 (1993).

[20] I. Ivanov, A. Mazur, and J. Pollmann, Surf. Sci. **92**, 365 (1980).

[21] J. Olde, G. Mante, H.-P. Barnscheidt, L. Kipp, J.-C. Kuhr, R. Manzke, M. Skibowski, J. Henk, and W. Schattke, Phys. Rev. B **41**, 9958 (1990).